Existence of Robust Edge States in Functionalized Germanene and Stanene Nanoribbons

Hunter, Jordyn; Wang Yaxian; Windl, Dr. Wolfgang
Department of Materials Science and Engineering, The Ohio State University Columbus, OH 43210 USA

ABSTRACT

Since the discovery of the quantum spin hall effect, there has been an increase in research in the field of 2D topological insulators, specifically in identifying and developing materials that exhibit the robust edge states characteristic of this topologically distinct state. Density functional theory calculations were performed to study the electronic properties of various functionalized germanene and stanene nanoribbons to identify potential topological insulators through the analysis of band structures and density diagrams. Band structure calculations show an opening of the band gap in GeI and SnI bulk structures with the inclusion of spin-orbit coupling, while $GeNH_2$ does not exhibit this property. The GeI and SnI nanoribbon band structures show further evidence of edges states, while the $GeNH_2$ nanoribbon structures do not. These results confirm that $GeNH_2$ is a predicted trivial insulator, but further research should be performed in straining the material in an attempt to induce a topological transition. We further confirm that GeI and SnI are topological insulators and have the potential to be utilized in the field of spintronics.

I. Background and Introduction

1.1 Topological Insulators

Since the discovery of the quantum hall state, which exists at low temperatures and in the presence of a strong magnetic field and characterized by an insulating bulk and chiral edge states, research of unique topological states occurring in 2D materials has increased over the past decade. Researchers specifically sought to find a material that exhibits conducting edge states without requiring the presence of an external magnetic field. Thus, the topological insulator, also known as the quantum spin hall state, was realized, and exists at room temperature and without an applied magnetic field due to the intrinsic magnetic field generated through spin-orbit coupling within the 2D material[1]. This unique state of matter is insulating in the bulk and conducting on the edges. However, these gapless edges do not carry solely charge, but are rather spin-polarized and extremely robust due to preservation of time-reversal symmetry, and thus are particularly useful in the field of spintronics[2].

1.2 Graphene and Analogous 2D Materials

The revolution of 2D materials began with the experimental discovery of graphene, a 2D planar sheet of carbon atoms. Its honeycomb structure and sp_2 hybridization, along with its virtually flat structure and linear electronic dispersion, produce a combination of unique mechanical and electronic properties.[3]

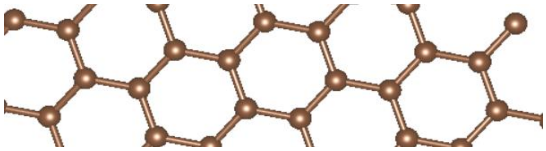

Figure 1. Hexagonal sp_2 hybridized graphene structure viewed from the c-axis.

However, due to graphene's small atomic number, it experiences weak spin-orbit coupling (SOC) which makes it an unlikely candidate for classification as a topological insulator. Further investigation into the world of 2D materials led to the realization of silicene, germanene, and stanene (tinene), which are also hexagonal lattices. Contrary to graphene, these structures experience buckling and sp_3 hybridization rather than sp_2, rendering them more chemically active.[4]

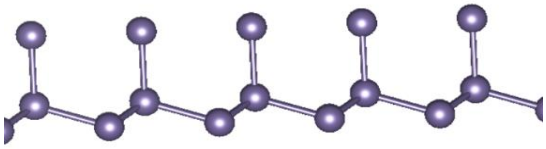

Figure 2. Buckled sp_3 hybridized structure exhibited by silicene, germanene, and stanene (viewed from the b-axis).

They also possess stronger SOC than graphene due to their larger atomic numbers, and thus are more likely to exhibit robust edge states.

1.3 Functionalization

The ability to tune the electronic properties of a material, such as the band gap, is highly favorable and has been observed when 2D structures are functionalized with certain ligands. Germanene for example, when functionalized with iodine, exhibits a decrease in its band gap width at the Γ point [(Figure 3(a) and 3(b)]. In the case of topological insulators, a smaller band gap is

preferred, as will be explained later, and thus functionalization is a valuable technique when attempting to develop materials to exhibit certain properties.

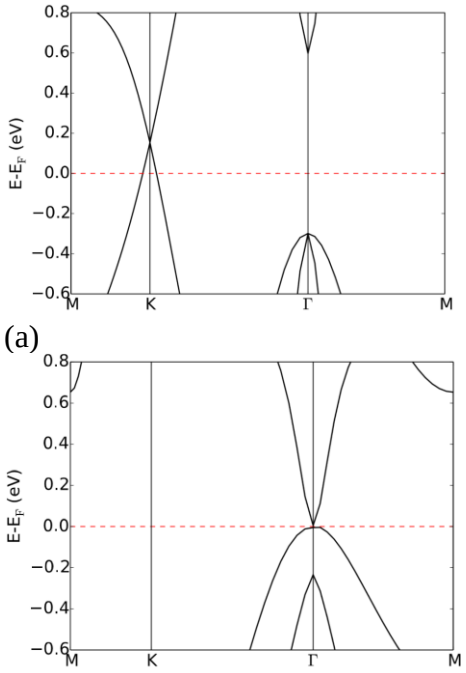

(a)

(b)

Figure 3. (a) Band structure of germanene sheet. (b) Band structure of germanene sheet functionalized with iodine.

Throughout this paper, we will explore various functionalized structures of germanene and stanene and analyze their unique electronic properties, determining whether they exhibit the topologically distinct characteristics of a topological insulator.

II. Models and Methods

All structures and unit cells were constructed using VESTA (Visualization for Electronic and Structural Analysis) software. Calculations were performed utilizing VASP (Vienna Ab-Initio Simulation Package) which implements

$$\frac{-\hbar^2}{2m}\nabla^2\Psi(\mathrm{r}) + V(r)\Psi(\mathrm{r}) = E\Psi(\mathrm{r})$$

Figure 4. Time-independent Schrödinger equation.

DFT (Density Functional Theory). Density functional theory is a quantum mechanical modeling method used to investigate the electronic structure of the ground state for a many body-system. It approximates the solution to the time-independent Schrödinger equation for a given system using electron density functionals. In the case of this system, structures were relaxed using the Perdew-Burke-Ernzerhof (PBE) functional, due to its accuracy and speed, (Figure 5) and a cutoff energy of 280 eV.

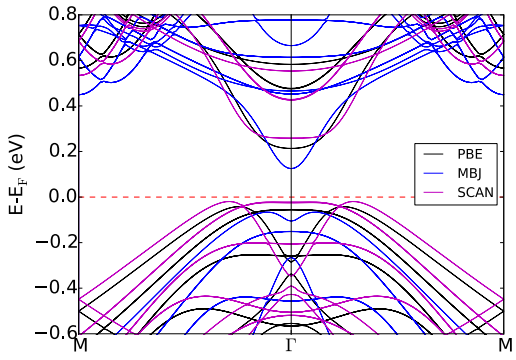

Figure 5. Comparison of various functionals implemented in DFT calculations. Shown using a GeI armchair nanoribbon band structure including spin-orbit coupling. Speed: PBE > MBJ > SCAN. Accuracy: SCAN > PBE > MBJ.

2.1 Iodine Functionalized Germanene

A bulk iodine functionalized germanene (GeI) unit cell was constructed using VESTA. Instead of using the primitive cell for the structure, a rectangular prism unit cell was created comparable to the nanoribbon unit cells that will be discussed in the next paragraph, as to allow an accurate comparison of band structures.

The unit cell had the dimensions a = 42.14Å, b = 8.11Å, c = 15.00Å after relaxation. These dimensions include the 5Å vacuum that was added above and below in the c-direction to prevent interactions between layers.

The iodine functionalized germanene zigzag nanoribbon (GeIZNR) unit cells were contsructed with various numbers of zags (N), which were numbered along the a-direction. A vacuum measuring 10Å was added to each side of the original bulk unit cell in the a-direction as to prevent any interactions between neighboring ribbons. The ribbon edges running along the the b-direction were passivated with hydrogen. A k-mesh of 1 x 6 x 1 was used, and after relaxation, the N = 12 unit cell had dimensions a = 59.79Å, b = 8.1Å, c = 15.00Å.

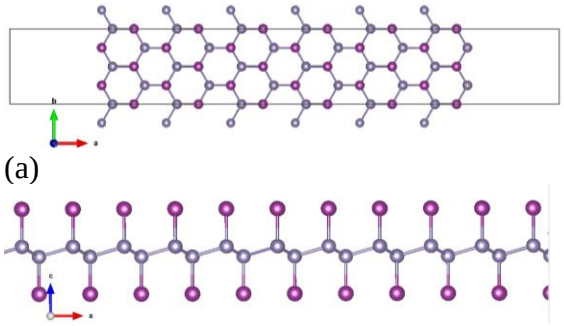

(a)

(b)

Figure 6. (a) GeIZNR unit cell with N = 12 viewed from the c-axis. (b) Viewed from the b-axis. Grey atoms represent germanium. Purple atoms represent hydrogen.

	Distance (Å)
Ge-Ge	2.44
Ge-I	2.57
Ge-H	1.52
$\Delta_{\text{buckling height}}$	0.69

Figure 7. Bond lengths and buckling height of pre-relaxed GeI structure.

These methods were repeated for a GeIZNR with N = 24.

2.2 Additional structures

The following structures were also constructed using VESTA. They were relaxed using a 1 x 6 x 1 k-mesh. A vacuum of 10Å was added to the nanoribbon unit cells on each side in the a-direction to prevent interaction between neighboring structures, and edges were passivated with hydrogen atoms. The 5Å vacuum was also added to every unit cell in the c-direction.

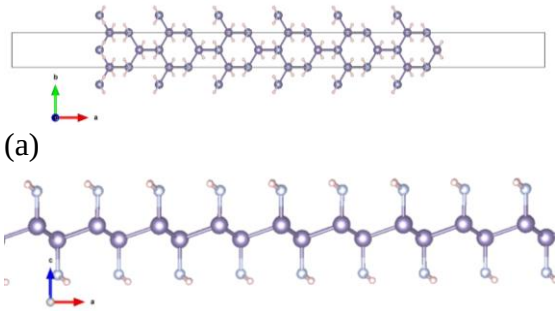

(a)

(b)

Figure 8. (a) Amide functionalized germanene zigzag nanoribbon ($GeNH_2$ZNR) unit cell with N = 12 viewed from the c-axis. (b) Viewed from the b-axis. Grey atoms represent germanium. Pale-blue atoms represent nitrogen. White atoms represent hydrogen.

	Distance (Å)
Ge-Ge	2.42
Ge-N	1.91
Ge-H	1.52
N-H	1.13
$\Delta_{\text{buckling height}}$	0.78
a_{12}	60.79
b_{12}	3.93
c_{12}	20.00
a_{bulk}	40.79
b_{bulk}	3.93
c_{bulk}	20.00

Figure 9. Characteristics of various $GeNH_2$ unit cells before relaxation takes place.

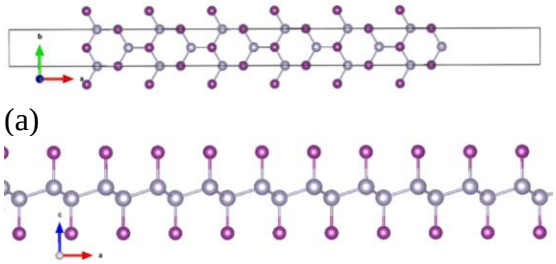

(a)

(b)

Figure 10. (a) Iodine functionalized stanene zigzag nanoribbon (SnIZNR) unit cell with N = 12 viewed from the c-axis. (b) Viewed from the b-axis. Grey atoms represent tin. Purple atoms represent iodine.

	Distance (Å)
Sn-Sn	2.83
Sn-I	2.70
Sn-H	1.70
$\Delta_{\text{buckling height}}$	0.85
a_{12}	68.53
b_{12}	4.67
c_{12}	19.33
a_{bulk}	48.53
b_{bulk}	4.67
c_{bulk}	19.33

Figure 11. Characteristics of various SnI unit cells before relaxation takes place.

III. Results and Discussion

3.1 Iodine Functionalized Germanene

First principle calculations were first carried out on the bulk GeI structures in order to analyze the SOC-induced band gap and investigate whether the material experiences band inversion.

3.1.1 Spin-orbit coupling (SOC)

Spin-orbit coupling is the interaction between the spin of an electron and the magnetic moment induced by its orbital motion. The electrons of opposite spin either align in parallel to the small orbital-generated magnetic field, or anti-parallel. This alignment causes a small change in energy between the electrons and thus splits the energy levels into spin-down and spin-up, and in some cases resulting in band gap openings and band inversion. This interaction is stronger in materials with more electrons and thus an increase in atomic number increases the strength of SOC.

3.1.2 Band inversion

Band inversion is a mechanism that is required to change a material's topological order. In the case of topological insulators, since they are topologically distinct, band inversion is a requirement. Essentially, band inversion occurs when the conduction and valence bands are inverted. In the case of semi-conductors, usually this involves an inversion of the s and p bands at the Γ point[5].

The band structures of bulk GeI with and without SOC were generated. In Figure 12 (a), in which SOC is not included in calculations, the band gap is extremely small, which is favorable in the case of topological insulators. Materials with smaller band gaps are more likely to exhibit band inversion and a SOC-induced band gap because SOC, although fairly strong in GeI, has a certain energy range in which it can influence the energy bands. The smaller the band gap, the more likely SOC will be influential. An analysis of Figure 12 (b), which included SOC, reveals that a band gap of about 0.3 eV was opened.

Another important characteristic illustrated in the band structure in Figure 12 (b) is the divet in one of the valence bands at the Γ point. Observing both a divet and opening of a band gap at this point is indicative that band inversion occurred, and most likely

occurred because the SOC was strong enough to split the energy of the bands so that one either exceeded or fell below in energy of one of its neighboring bands. However, the band structure plots are unable to illustrate which energy bands were inverted (e.g. s, p, etc.); other methods should be used in the future to analyze the orbital contributions to each band to confirm which energy bands were specifically inverted.

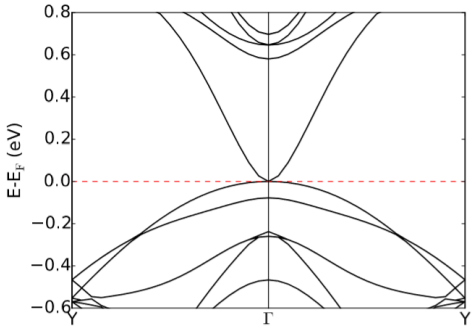

(a)

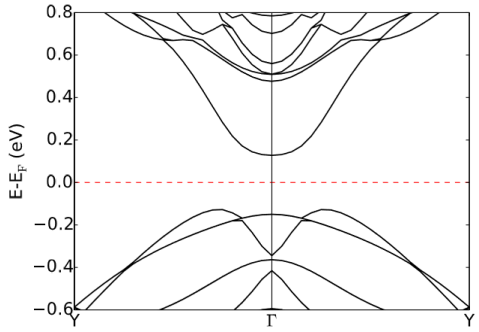

(b)

Figure 12. Band structures of bulk GeI without (a) and with (b) SOC.

Additional calculations were performed on the GeI nanoribbons to analyze the edge states. With the introduction of SOC into calculations in Figure 13 (b), there appears to be band crossing at the Fermi-level, and thus this material is predicted to exhibit conducting edge states.

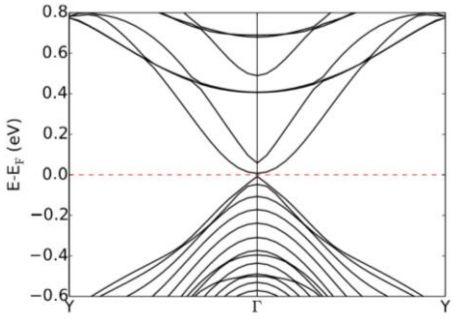

(a)

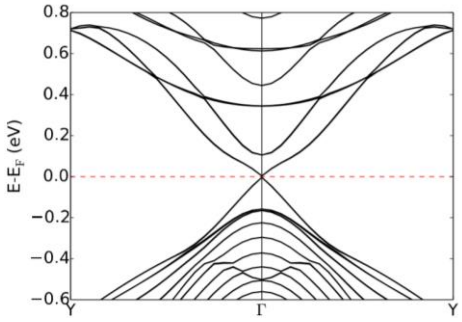

(b)

Figure 13. Band structures of GeIZNR with N = 12 without (a) and with (b) SOC.

To further confirm these edge states, partial charge density diagrams were generated for several GeI nanoribbon structures at the Γ point for the two specific bands that are participating in the band crossing (Figure 14). These diagrams reveal that the electrons within these crossing bands are localized along the edges, and thus further confirms the existence of edge states.

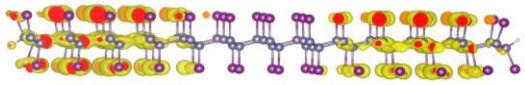

(a)

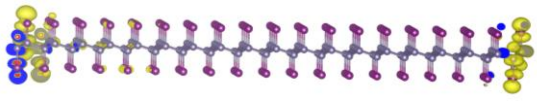

(b)

Figure 14. Partial charge density calculated at the Γ point for GeIANR with (a) N = 12 and (b) N = 18.

The band inversion, the band gap opening at the Fermi-level, and the existence of edge states indicate that GeI could potentially be a topological insulator if synthesized.

3.2 Iodine Functionalized Stanene

Similar calculations were performed for SnI as were done for GeI. First principle calculations were carried out to generate band structures and first analyze the band gap induced by SOC. In Figure 15 (b), again, we see a small band gap. The band gap is small enough and the SOC effect is strong enough to open a significant band gap of around 0.35 eV.

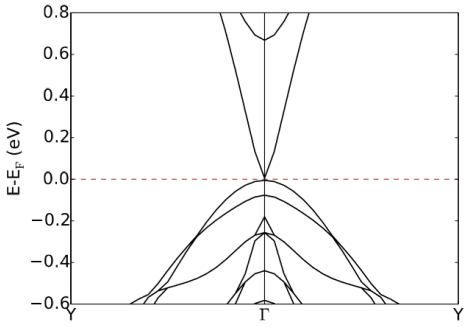

(a)

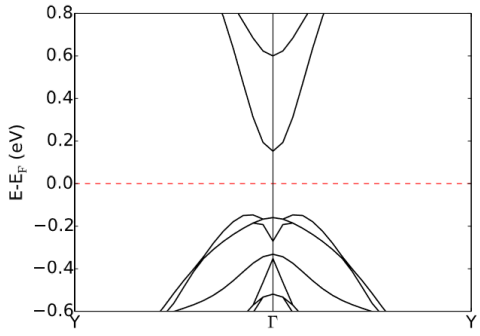

(b)

Figure 15. Band structures of bulk SnI without (a) and with (b) SOC.

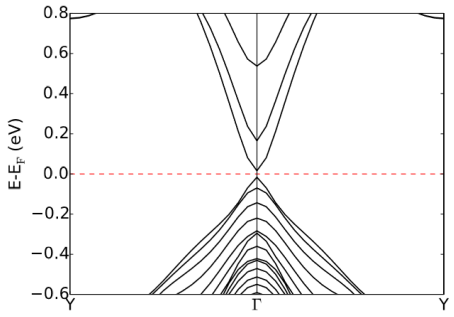

(a)

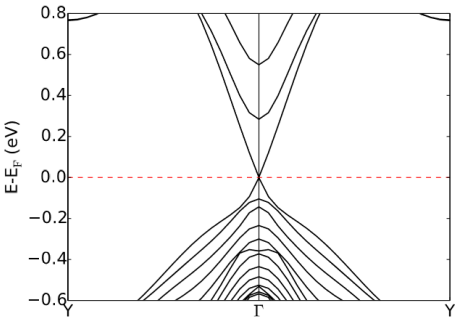

(b)

Figure 16. Band structures of SnIZNR with N = 12 without (a) and with (b) SOC.

Further calculations were performed on various SnI zigzag nanoribbons to analyze the electronic properties of the edges. In Figure 16 (b), with the inclusion of SOC, the band crossing is apparent at the Fermi-level and thus, the robust edge states are predicted to exist in SnI nanoribbons.

In addition, a projected density of states plot was generated to analyze which specific orbitals contributed to the edge states (Figure 17). Projected density of states is similar to the density of states of a system, in that it also describes the number of states available at a certain energy level; however, it also provides insight into which orbitals contributed to the density of states, which could be used in the future to determine which orbitals participated in band inversion for the bulk SnI band structure.

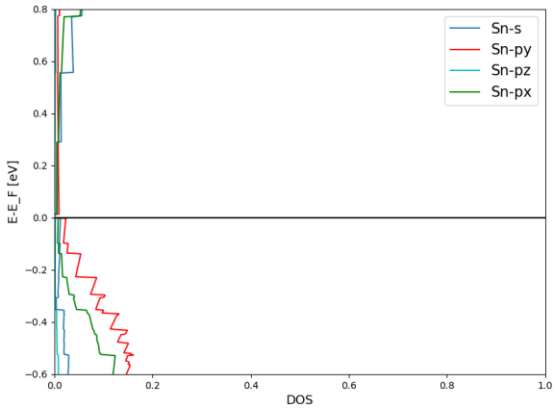

Figure 17. Projected density of states contributions around the Fermi level in a SnIZNR with N = 12 with the inclusion of SOC.

3.3 Amide Functionalized Germanene

First principle calculations were performed for $GeNH_2$ structures to analyze the band gaps and edge states.

Bulk band structures were generated for $GeNH_2$. In Figure 18, there is no noticeable different between the band structure plot generated with SOC and that calculated without SOC. Due to this result, it is predicted that the band gap of bulk $GeNH_2$ is far too large for SOC to influence the energy bands, and thus it is predicted to be a trivial insulator.

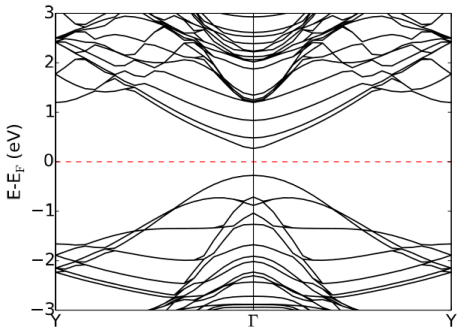

(a)

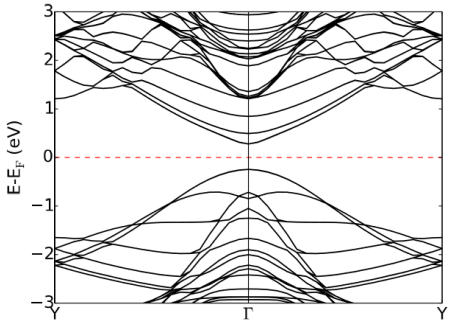

(b)

Figure 18. Band structures of bulk $GeNH_2$ without (a) and with (b) SOC.

Further calculations were performed to confirm this prediction. Band structure plots for $GeNH_2$ nanoribbons were generated (Figure 19), and it is apparent that there are no bands crossing the Fermi-level, and thus edge states do not exist for this structure.

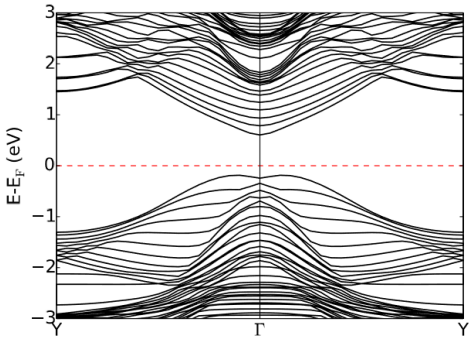

(a)

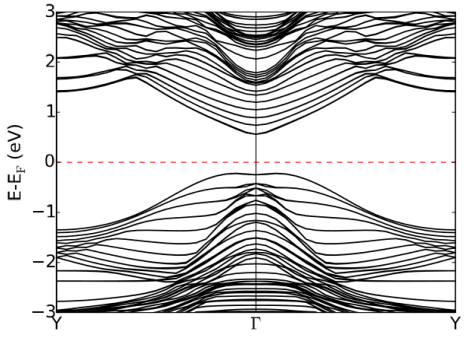

(b)

Figure 19. Band structures of $GeNH_2$ZNR with N = 12 without (a) and with (b) SOC.

The partial density calculations (Figure 20) illustrate that there is no localization of charge in the bands near the Fermi-level. This further confirms that the edge states do not exist.

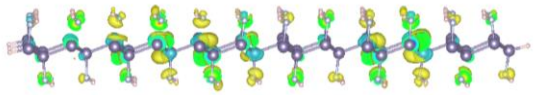

Figure 20. Partial density calculated at the Γ point in $GeNH_2$ZNR with N = 12.

Lastly, as to allow insight into the orbital contributions near the Fermi-level, projected density of states plots were generated and illustrate that the s-orbital dominates above the Fermi-level, while the p_y-orbital dominates below. This information could be further utilized to determine why this material does not exhibit robust edge states, and further calculations should be performed using projected density of states to confirm that band inversion did not occur in bulk $GeNH_2$.

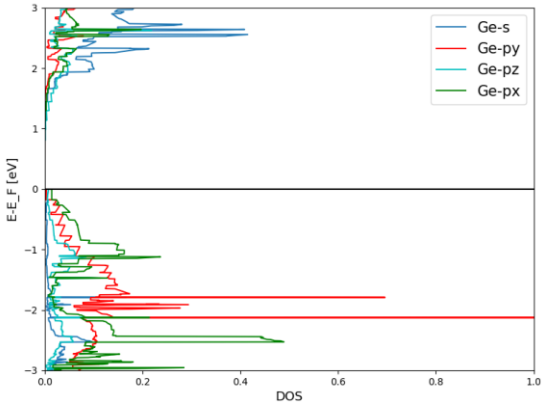

Figure 21. Projected density of states around the Fermi level in $GeNH_2$ZNR with N = 12 and with the inclusion of SOC.

IV. Conclusions

After having analyzed the various band structure plots and density diagrams for each material, it is confirmed that GeI and SnI are indeed topological insulators since they exhibit both the bulk band gap opening due to SOC and the unique edge states crossing the Fermi-level in their nanoribbon band structures. On the other hand, for the $GeNH_2$ structure, SOC appeared to have no effect on the bulk band gap and no edge states were apparent in nanoribbon calculations. Based on the band structure plots, it was concluded that the band gap was too large for SOC to influence the energy levels, and thus it is a predicted trivial insulator rather than a topological insulator.

Further research should be done in investigating the band inversion mechanism. Since band inversion is essential to modify a material's topological order, and thus essential in topological insulators, it would be very useful to understand its exact causes. In some cases, as is in the case of the materials described throughout this paper, band inversion is induced by SOC; however, there have been cases in which materials such as GeH, which are not topological insulators in their equilibrium state, can be stretched to induce band inversion and thus change the their topological order[6].

Furthermore, since our results predicted $GeNH_2$ to be a trivial insulator, more research into strained $GeNH_2$ should be performed to attempt to induce band inversion and thus convert it to a topological insulator. This would be valuable since $GeNH_2$ has been synthesized and thus it would be ready for immediate application. Other systems which have been synthesized should also be investigated; rather than focusing solely on the theoretical aspect of topological insulators, researchers should work backwards by choosing materials that are able to be synthesized, and then performing further calculations to determine their

candidacy for unique topological properties.

V. Acknowledgments

I would like to thank Dr. Wolfgang Windl for providing me with an interesting and novel research topic. Furthermore, I would like to thank my graduate student mentor, Yaxian Wang, for teaching me all that she has this summer and taking the time and patience to aid in my skill development.

Lastly, I would like to thank Michelle McCombs and the other REU coordinators for organizing the program this summer. The experience was truly invaluable, and I will take all that I have learned this summer with me into the future.

Funding for this project was provided by the National Science Foundation.

VI. Footnotes, Endnotes and References

[1] Lee, M. M., Teuscher, J., Miyasaka, T., Murakami, T. N., & Snaith, H. J. (2012). Quantum Spin Hall Effect and Topological Phase Transition in HgTe Quantum Wells. Science, 338(November), 643–646. http://doi.org/10.5061/dryad.9g182

[2] Moore, J. E. (2010). The birth of topological insulators. Nature, 464(7286), 194–198. http://doi.org/10.1038/nature08916

[3] Neto, A. H. C., Guinea, F., Peres, N. M. R., Novoselov, K. S., & Geim, A. K. (2007). The electronic properties of graphene, 81(March). http://doi.org/10.1103/RevModPhys.81.109

[4] Balendhran, S., Walia, S., Nili, H., Sriram, S., & Bhaskaran, M. (2015). Elemental analogues of graphene: Silicene, germanene, stanene, and phosphorene. Small. http://doi.org/10.1002/smll.201402041

[5] Zhu, Z., Cheng, Y., & Schwingenschlögl, U. (2012). Band inversion mechanism in topological insulators: A guideline for materials design. Physical Review B - Condensed Matter and Materials Physics, 85(23), 1–5. https://doi.org/10.1103/PhysRevB.85.235401

[6] Si, C., Liu, J., Xu, Y., Wu, J., Gu, B. L., & Duan, W. (2014). Functionalized germanene as a prototype of large-gap two-dimensional topological insulators. Physical Review B - Condensed Matter and Materials Physics, 89(11), 1–5. https://doi.org/10.1103/PhysRevB.89.115429